Computational Materials Science 172 (2020) 109315

Contents lists available at ScienceDirect

Computational Materials Science

journal homepage: www.elsevier.com/locate/commatsci

Highly accurate prediction of material optical properties based on density functional theory

Mitsutoshi Nishiwaki, Hiroyuki Fujiwara*

Department of Electrical, Electronic and Computer Engineering, Gifu University, 1-1 Yanagido, Gifu 501-1193, Japan

ARTICLE INFO

Keywords:
First principles calculation
Absorption coefficient calculation
Dielectric function calculation
Extinction coefficient calculation
PHS method
Kramers-Kronig integration

ABSTRACT

Theoretical material investigation based on density functional theory (DFT) has been a breakthrough in the last century. Nevertheless, the optical properties calculated by DFT generally show poor agreement with experimental results particularly when the absorption-coefficient (α) spectra in logarithmic scale are compared. In this study, we have established an alternative DFT approach (PHS method) that calculates highly accurate α spectra, which show remarkable agreement with experimental spectra even in logarithmic scale. In the developed method, the optical function estimated from generalized gradient approximation (GGA) using very high-density *k* mesh is blue-shifted by incorporating the energy-scale correction by a hybrid functional and the amplitude correction by sum rule. Our simple approach enables high-precision prediction of the experimental α spectra of all solar-cell materials (GaAs, InP, CdTe, $CuInSe_2$ and $Cu_2ZnGeSe_4$) investigated here. The developed method satisfies the requirements of high accuracy and low computational cost simultaneously and is superior to conventional GGA, hybrid functional and GW methods.

1. Introduction

Prediction of material optical properties based on density functional theory (DFT) has been a revolutionary technique that allows quite effective optical-material searches even without forming materials experimentally [1–4]. The DFT methods for optical-function calculation have already been established [5–9] and a vast amount of optical spectra deduced from DFT calculations have been reported [1–15]. Nevertheless, a critical view point that has been lacking in conventional DFT optical-function calculations is the justification of calculation results. In particular, calculated DFT spectra vary rather significantly with the choice of the approximation method [8–10]. Thus, the DFT calculation results need to be verified based on experimental spectra.

So far, optical-function calculations by DFT have mainly been justified by the comparison with experimental dielectric functions ($\varepsilon = \varepsilon_1 - i\varepsilon_2$) in linear scale [4–9]. In photovoltaic device simulations, however, the absorption-coefficient (α) spectrum in logarithmic scale ($\alpha = 10^2$–$10^6\ cm^{-1}$) is generally required [16,17]. When the logarithmic α spectra obtained from experiment and DFT calculation are compared, the agreement is generally poor and the difference between the theoretical and experimental values often reaches almost one order of magnitude [10,15]. Accordingly, there is a strong requirement for establishing a DFT calculation method that can accurately predict α spectra in conventional logarithmic scale.

We previously found that very-high-density *k* mesh calculations are essential to accurately reproduce the α variation of various solar cell materials particularly in the band gap (E_g) region [13]. When α spectra calculated within generalized gradient approximation (GGA) [18] using high-density *k* mesh are blue-shifted toward higher energy to compensate the underestimated E_g contribution in GGA, the DFT and experimental spectra show remarkable agreement [13]. Later, it was suggested to shift the GGA-calculated α spectra using E_g values estimated from hybrid-functional DFT calculations [19]. However, the validity of such a method has not been discussed properly.

In this study, to realize a highly accurate prediction method of material α spectra, we have developed a quite general DFT calculation scheme, in which ε_2 spectra calculated by GGA using very high *k*-mesh density are blue-shifted toward more accurate energy scale determined by a hybrid functional (HSE06) [20,21] while performing the amplitude correction simultaneously based on sum rule [22]. A key feature of our method is the combination of GGA within the Perdew-Burke-Ernzerhof scheme (PBE) [18] with HSE06 and sum rule and, from this PHS approach (PBE + HSE06 + Sum rule), the dielectric function and optical constants (refractive index *n*, extinction coefficient *k* and α) are readily obtained in a consistent manner. As a result, we find that the α spectra of representative solar cell materials [GaAs, CdTe, InP, $CuInSe_2$ (CISe), and $Cu_2ZnGeSe_4$ (CZGSe)], calculated by the developed PHS method,

* Corresponding author.
E-mail address: fujiwara@gifu-u.ac.jp (H. Fujiwara).

https://doi.org/10.1016/j.commatsci.2019.109315
Received 11 July 2019; Received in revised form 24 September 2019; Accepted 25 September 2019

show remarkable agreement with the experimental spectra in a wide α range of 10^2–10^6 cm^{-1}. Our approach provides an ideal method for accurate prediction of overall material optical properties with low computational cost, which can be incorporated directly into optical device simulations.

2. PHS method

Fig. 1 explains the calculation procedure of the PHS method developed in this study. Here, as an example, the calculation of a GaAs dielectric function is shown. In our approach, the ε_2 spectrum of the dielectric function is calculated first using very high k-mesh density within GGA-PBE. As known well [23], E_g is seriously underestimated when DFT calculations are performed within PBE. To compensate this underestimated E_g contribution, the calculated PBE ε_2 spectrum ($\varepsilon_{2,PBE}$) is blue-shifted. In this energy shift, the E_g correction value (ΔE_g) is determined according to $\Delta E_g = E_{g,HSE} - E_{g,PBE}$, where $E_{g,HSE}$ and $E_{g,PBE}$ represent the E_g values estimated from HSE06 and PBE, respectively.

When the ε_2 spectrum is shifted toward higher energy, however, it is necessary to satisfy sum rule [22], given by

$$\int E\varepsilon_2(E)dE = \text{const.} \tag{1}$$

If the ε_2 spectrum is shifted toward higher energy by ΔE_g, sum rule requires that

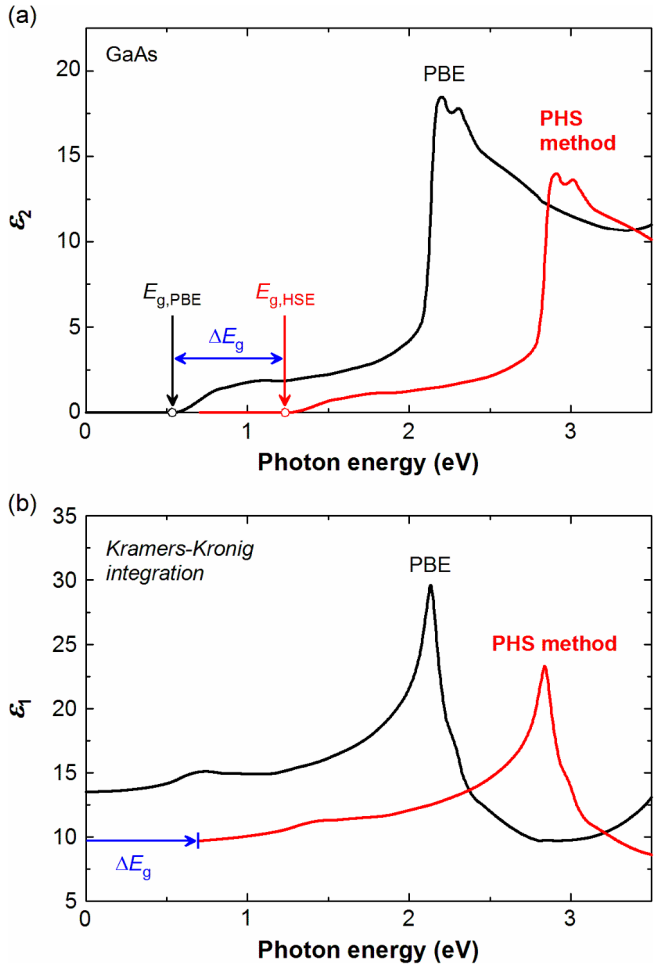

Fig. 1. Calculation of (a) ε_2 spectrum and (b) ε_1 spectrum for GaAs based on the PHS method. In (a), the determination of a E_g correction value ($\Delta E_g = E_{g,HSE} - E_{g,PBE}$) is indicated. The ε_1 spectrum is obtained from Kramers-Kronig integration of (a).

$$\int E\varepsilon_2(E)dE = \int (E + \Delta E_g)\varepsilon_{2,Shift}(E + \Delta E_g)dE, \tag{2}$$

where $\varepsilon_{2,Shift}$ shows the shifted ε_2 spectrum. If the prefactors of E and $E + \Delta E_g$ in the above equation are taken as constants, we obtain

$$\int \varepsilon_{2,Shift}(E + \Delta E_g)dE = f\int \varepsilon_2(E)dE, \tag{3}$$

where $f = E/(E + \Delta E_g)$. In order for Eq. (2) to be satisfied, therefore, the amplitude of $\varepsilon_{2,Shift}$ needs to be reduced by a factor of f [16] and, by applying this principle, we obtain $\varepsilon_{2,Shift}(E + \Delta E_g) = f\varepsilon_2(E)$. If we convert the E axis of this equation using $E + \Delta E_g \rightarrow E$ (i.e., $E \rightarrow E - \Delta E_g$) and assume that $\varepsilon_2(E) = \varepsilon_{2,PBE}(E)$, the ε_2 spectrum of the PHS method [$\varepsilon_{2,PHS}(E)$] is calculated by setting $\varepsilon_{2,PHS}(E) = \varepsilon_{2,Shift}(E)$ as follows:

$$\varepsilon_{2,PHS}(E) = \frac{E - \Delta E_g}{E}\varepsilon_{2,PBE}(E - \Delta E_g). \tag{4}$$

In Fig. 1(a), the calculation results of $\varepsilon_{2,PHS}$ and $\varepsilon_{2,PBE}$ are shown. The ε_1 contribution of the PHS method ($\varepsilon_{1,PHS}$) can then be obtained from Kramers-Kronig integration [22]:

$$\varepsilon_{1,PHS}(E) = 1 + \frac{2}{\pi}P\int_0^\infty \frac{E'\varepsilon_{2,PHS}(E')}{E'^2 - E^2}dE'. \tag{5}$$

The results of $\varepsilon_{1,PHS}$ and $\varepsilon_{1,PBE}$ are compared in Fig. 1(b). From ($\varepsilon_{1,PHS}$, $\varepsilon_{2,PHS}$), n_{PHS} and k_{PHS} are determined by conventional formula:

$$n_{PHS} = \{[\varepsilon_{1,PHS} + (\varepsilon_{1,PHS}^2 + \varepsilon_{2,PHS}^2)^{1/2}]/2\}^{1/2}, \tag{6}$$

$$k_{PHS} = \{[-\varepsilon_{1,PHS} + (\varepsilon_{1,PHS}^2 + \varepsilon_{2,PHS}^2)^{1/2}]/2\}^{1/2}. \tag{7}$$

Finally, the α spectrum of the PHS method is deduced as $\alpha_{PHS} = 4\pi k_{PHS}/\lambda$.

3. DFT calculation

The DFT calculations were performed using Advance/PHASE and the Vienna *Ab initio* Simulation Package (VASP) [24]. For the calculations of GGA within PBE, the Advance/PHASE software was employed, while the VASP software was applied for HSE06 calculations. For the DFT calculations of zincblende crystals (GaAs, CdTe, InP), two-atom primitive cells were used, while eight-atom primitive cells were employed for CISe and CZGSe. The structural optimization of all the crystals was made by HSE06 using a plane-wave cutoff energy of 455 eV and the structures obtained from this procedure were applied for all the optical function calculations implemented by PBE and HSE06. For our DFT calculations, a tetrahedron smearing method has been adopted.

The optical-function calculations using PBE were made based on a method developed by Kageshima et al. [25]. In this calculation, plane-wave ultrasoft pseudopotential and tetrahedron methods were adopted. In addition, for Cu-containing compounds (CISe and CZGSe), the onsite Coulomb interaction was considered for the Cu 3*d* state [26] with an effective energy of $U_{eff} = 3$ eV. Unless otherwise noted, for the PBE calculations, we used a highly dense 30 × 30 × 30 k mesh for GaAs, CdTe and InP, whereas a 16 × 16 × 16 k mesh was employed for CISe and CZGSe [13,14]. The above k mesh densities were chosen so that the k mesh density in the k space becomes less than 0.1 $Å^{-1}$. We previously confirmed that this k mesh density provides satisfactory agreement with experimental results [13,14].

The optical-function calculation based on HSE06 was implemented for GaAs using a 30 × 30 × 30 k mesh, unless otherwise noted. In this case, the k-space integration was made based on a Γ-centered Monkhorst-Pack method. In the default setting of the VASP software, the calculated optical spectrum is broadened with a broadening parameter (complex shift) of $\eta = 0.1$. To avoid this, we have calculated the HSE06 ε_2 spectra by applying $\eta = 0$ and obtained the corresponding ε_1 spectra using Kramers-Kronig integration.

4. Results and discussion

Fig. 2 shows (a) the ε_2 spectra and (b) the ε_1 spectra of GaAs obtained from experiment (open circles) and the DFT calculations (solid lines). For the DFT results, those obtained applying PBE, HSE06 and the PHS method are shown. The experimental spectrum was taken from Ref. [17]. Since E_g is seriously underestimated in PBE, the whole PBE spectrum is red-shifted, compared with the experimental spectrum. In contrast, the HSE06 calculation provides a better fitting to the experimental spectrum and the optical transition energies observed in the experimental spectrum are reproduced well, as reported previously [9]. When the PHS method is applied, we obtain the ε_2 spectrum shown by the red line in Fig. 2(a) ($\Delta E_g = 0.705$ eV), which is quite similar to the HSE06 result. As shown in Fig. 2(b), the ε_1 spectrum calculated by the PHS approach provides satisfactory agreement with the experimental result. In the PHS and HSE06 calculation results, the ε_2 peak amplitude in the high energy region ($E \sim 3$ eV) is lower than the experimental value, suggesting the underestimation of the joint density of states or the oscillator strength in the optical transition. In the calculation of a CdTe zincblende crystal, a similar trend has also been confirmed [13].

Fig. 3 shows the variation of the calculated GaAs α spectrum with the k-mesh density in (a) the PHS method and (b) HSE06 method. In this figure, the DFT results (solid lines) are compared with the experimental α spectrum [17]. It can be seen that, for both PHS and HSE06 methods, the spectral calculation using a very high mesh density is vital for the accurate reproduction of the experimental α spectrum in logarithmic scale. This is based on the fact that the light absorption in the E_g region is highly localized near the Γ point in the Brillouin zones in conventional tetragonal-based semiconductors [13,27] and the precise k-space calculation particularly around the Γ point is necessary to reproduce the band-edge optical transition accurately [13]. As a result, the agreement with the experimental α improves significantly as the k-mesh density is increased. In particular, the result of Fig. 3 shows clearly that the band-edge α is underestimated seriously when a low k-mesh density is employed in the HSE06 calculation.

Fig. 4 further shows the effect of the HSE06 broadening parameter (η) on the α spectrum. The experimental spectrum and the HSE06 spectrum of $\eta = 0$ are consistent with those shown in Fig. 3(b). As shown in Fig. 4, if a default broadening parameter of $\eta = 0.1$ is applied in the HSE06 calculation, nominal light absorption occurs even below E_g. This is artifact caused by smoothening of the calculated ε_2 spectrum and such an artifact needs to be eliminated by setting η to zero.

Fig. 5 summarizes the GaAs α spectra calculated by the PHS, HSE06 and GW methods. The α spectrum estimated from GW is adopted from Ref. [8]. For the PHS and HSE06 results, those obtained using a $30 \times 30 \times 30$ k mesh, shown in Fig. 3, are indicated. As confirmed from Fig. 5, the DFT α spectra obtained using the PHS and HSE06 methods provide quite good agreement with the experimental spectrum. In the GW spectrum, the overall experimental spectrum is reproduced well but the agreement in the E_g region is quite inferior. It should be emphasized that the band-edge α has a significant impact on the operation of solar cell devices [16,28] as the photocarrier collection becomes more difficult in the near-E_g region due to the increase in the light penetration depth ($d_p = 1/\alpha$). Thus, accurate prediction of the band-edge α is of paramount importance particularly when DFT spectra are applied

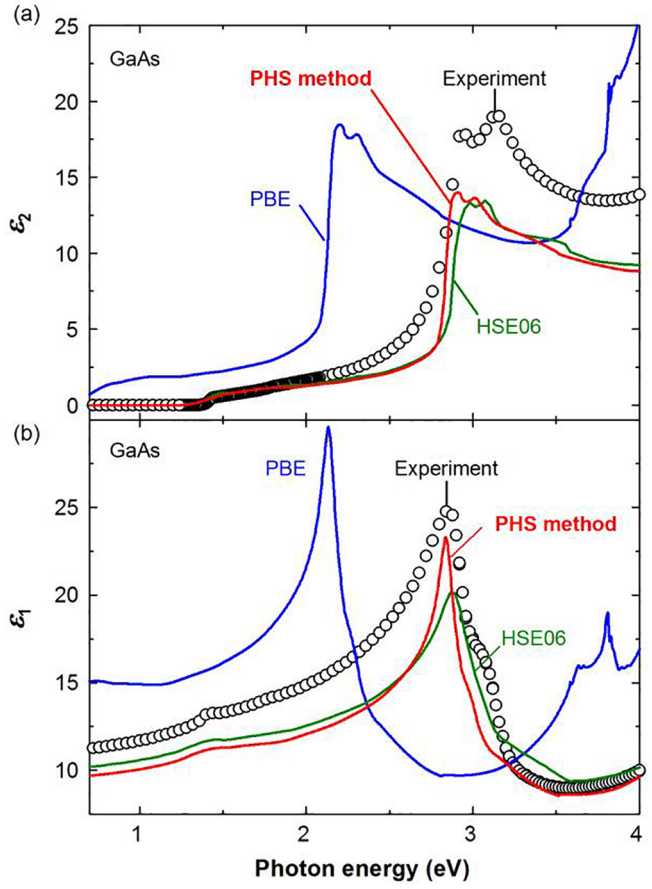

Fig. 2. (a) ε_2 spectra and (b) ε_1 spectra of GaAs obtained from experiment (open circles) and theoretical DFT calculations (solid lines). For the calculations, the results determined by PBE, HSE06, and the developed PHS method are shown. The experimental data were taken from Ref. [17].

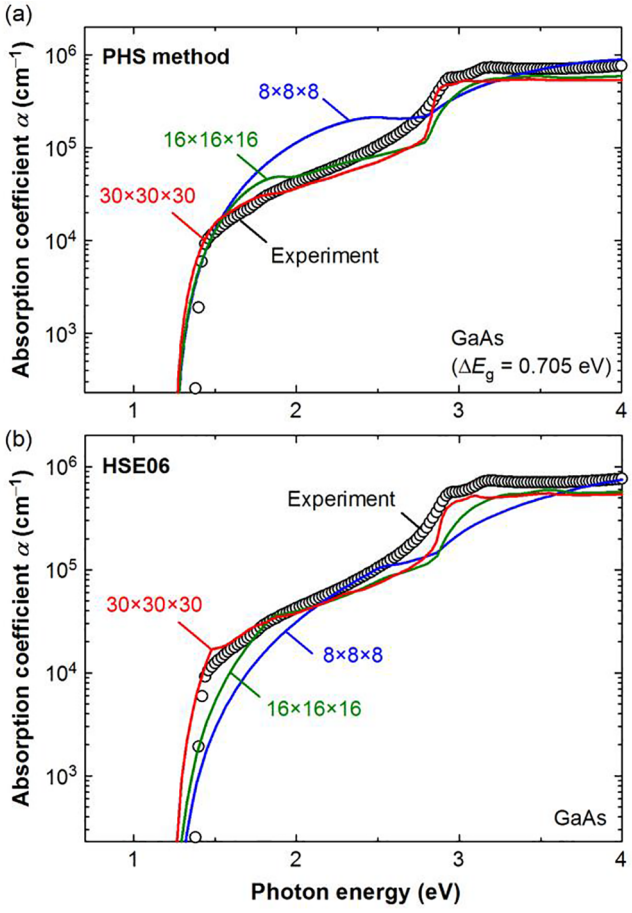

Fig. 3. GaAs α spectra calculated using different k-mesh densities based on (a) the PHS method and (b) the HSE06 method (sold lines). The experimental result (open circles) is taken from Ref. [17]. The ΔE_g in (a) represents the energy-shift value of the PBE spectra ($\Delta E_g = E_{g,HSE} - E_{g,PBE}$).

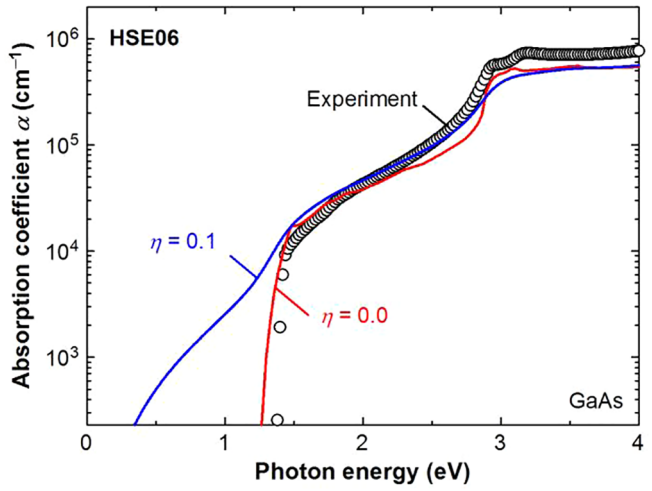

Fig. 4. GaAs α spectra calculated by HSE06 using different broadening parameters (η). The solid lines show the calculated results, whereas the open circles indicate the experimental result [17]. The DFT spectrum of $\eta = 0$ and the experimental spectrum are consistent with those of Fig. 3(b). When η was set to zero, the corresponding ε_1 spectrum was calculated from the ε_2 spectrum by applying Kramers-Kronig integration.

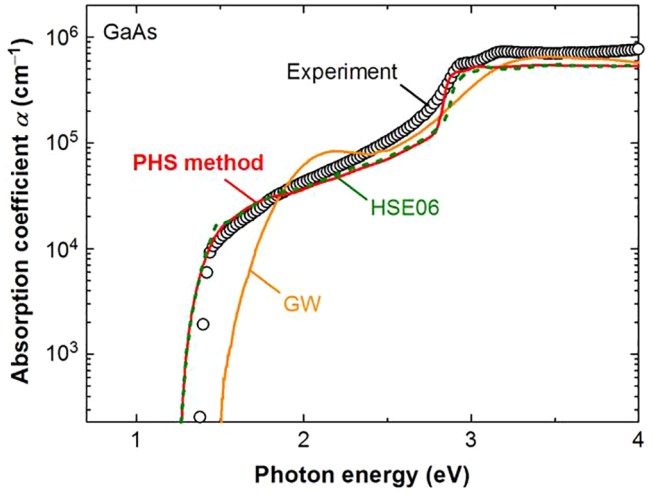

Fig. 5. Comparison of GaAs α spectra calculated by the PHS (red line), HSE06 (green dotted line) and GW (orange line) methods. The GW spectrum is adopted from Ref. [8]. The experimental result (open circles) is taken from Ref. [17].

directly to optical device simulations.

Although the PHS and HSE06 methods provide similar reproducibility for the experimental spectrum, our PHS approach allows the drastic reduction of calculation time. In particular, in the PHS method, since the high-density k mesh calculation is implemented using a rather simple PBE approximation, the calculation cost is far lower, compared with the HSE06 method. For example, the calculation time of the dielectric function of a GaAs crystal (two-atom primitive cell) using PBE is 0.1 s per k-point (0.75 h in total for a 30 × 30 × 30 k mesh), while a similar calculation using HSE06 results in 4.8 s per k-point (36 h in total for the same 30 × 30 × 30 k mesh). In general, the total calculation time increases drastically when the number of atoms in a primitive cell increases; thus, the accurate α calculation becomes quite difficult when HSE06 is applied for more complicated crystal structures. Moreover, the calculation cost of the GW method is even higher than HSE06 and the application of high-density k mesh calculation is generally limited in the case of GW. As a result, only the developed PHS method satisfies the criteria of high accuracy and low computational cost simultaneously.

As mentioned above, sum rule is incorporated in our PHS method. When the ε_2 spectrum calculated by PBE is shifted toward higher energy without considering sum rule, α is overestimated notably in the E_g region (supplementary material, Fig. 1). Accordingly, the incorporation of sum rule and the following Kramers-Kronig integration are essential. On the other hand, when the α spectrum calculated by PBE is simply blue-shifted by ΔE_g, we obtain a spectrum similar to the one calculated from the PHS method (supplementary material, Fig. 2). Thus, although the rigorous approach of the PHS method is preferable, the shifted PBE α spectrum could also be adopted [13].

We have applied the PHS method for the α calculation of other solar cell materials. Fig. 6 shows the α spectra of (a) CdTe, (b) InP, (c) CISe and (d) CZGSe, obtained from experiment [14,17,29] and the calculations using the PHS method. The ΔE_g values determined from the calculations are also indicated. In Fig. 6, all the calculated results show remarkable overall agreement with the experimental spectra, confirming the universality of our PHS approach.

To justify our method further, we have calculated the band structures of the solar cell materials. Fig. 7 compares the band structures of (a) CdTe, (b) InP, (c) CISe and (d) CZGSe, obtained from PBE and HSE06. In the PBE results of Fig. 7, all the conduction band positions were shifted upward by ΔE_g so that E_g becomes consistent with that obtained from HSE06 (scissor operation [30]). As known well [31], the underestimation of E_g within PBE originates from the assumption that only non-interacting single particle is considered in the E_g estimation; however, the variations of individual conduction and valence bands deduced from PBE are still accurate. When the PBE conduction bands are shifted, therefore, all the PBE bands show excellent agreement with the bands approximated by HSE06 [13]. A similar good agreement has also been observed for GaAs (supplementary material, Fig. 3). Since the optical transitions are derived essentially from the band structures, the result of Fig. 7 verifies that the underestimated E_g contribution observed in the PBE spectra can be corrected by simply shifting the PBE spectra toward higher energies using ΔE_g. In other words, the validity of our PHS method can be confirmed by simply comparing the conduction-band-shifted PBE band structure with the HSE06 band structure. Since the band-edge light absorption of tetragonal-based semiconductors is determined primarily by the optical transition from the first valence band to the first conduction band [27], the agreement near the valence band maximum and conduction band minimum is particularly important.

5. Conclusion

We have developed a new DFT approach that can accurately predict material α spectra in logarithmic scale. In this method, the ε_2 spectrum calculated from the PBE functional using very high-k mesh density is blue-shifted and the underestimated E_g contribution in PBE is corrected using the energy scale determined by HSE06 calculation, while the ε_2 amplitude is corrected by applying sum rule. We have applied the developed method for the α calculations of five solar cell materials (GaAs, InP, CdTe, $CuInSe_2$ and $Cu_2ZnGeSe_4$) and the α spectra calculated by our method provide remarkable agreement with those observed experimentally. Our scheme realizes the requirements of high accuracy and low calculation cost simultaneously and allows the direct application of calculated DFT optical spectra to various optical device simulations.

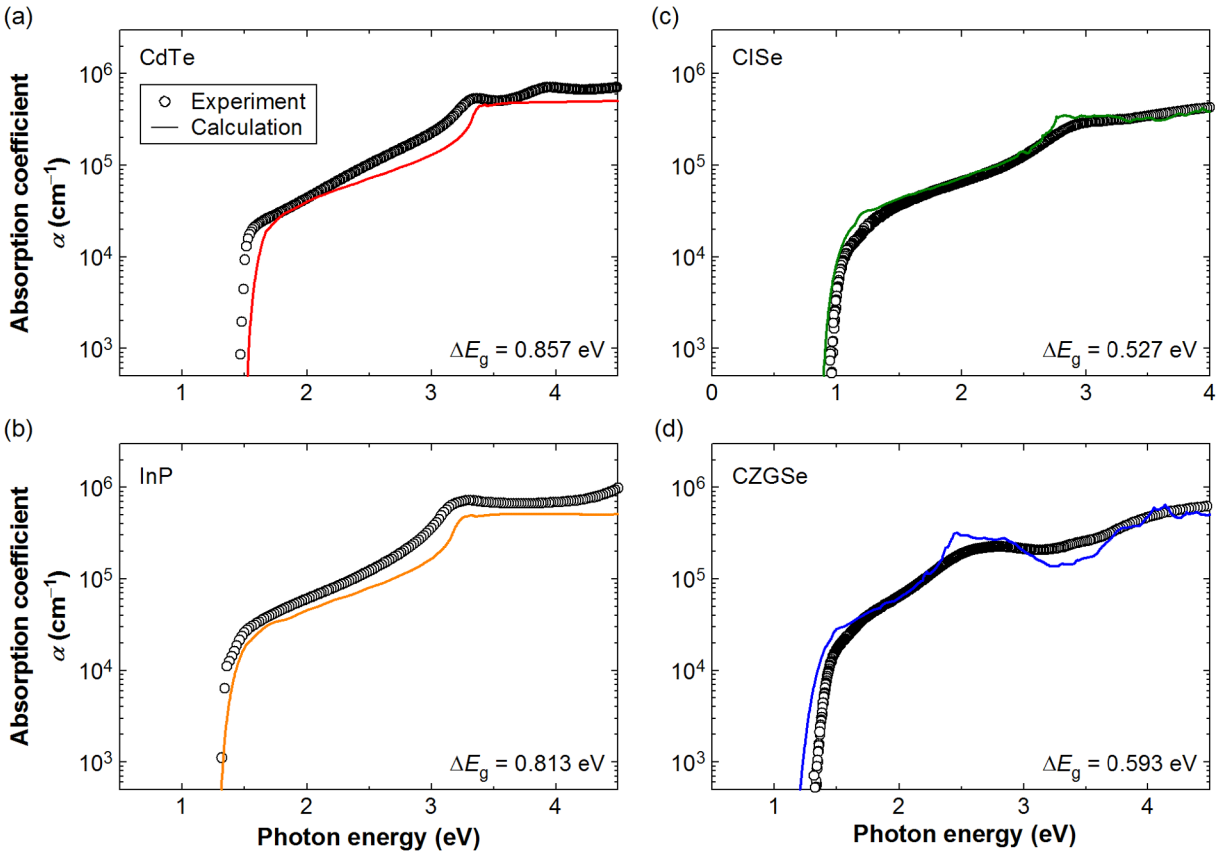

Fig. 6. α spectra of (a) CdTe, (b) InP, (c) CISe and (d) CZGSe, obtained from experiment (open circles) and the calculations using the PHS method (solid lines). The ΔE_g values of each spectrum are also indicated. The experimental data were adopted from Refs. [14], [17] and [29].

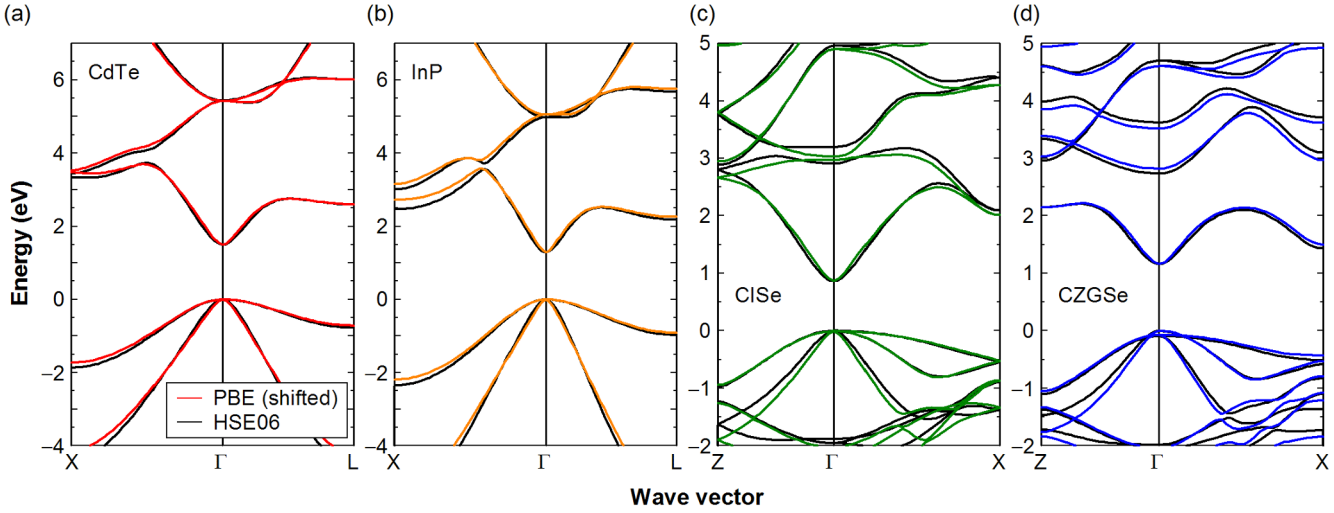

Fig. 7. Band structures of (a) CdTe, (b) InP, (c) CISe and (d) CZGSe calculated using PBE and HSE06. In the PBE results, all the conduction band positions were shifted upward by ΔE_g.

CRediT authorship contribution statement

Mitsutoshi Nishiwaki: Conceptualization, Formal analysis. **Hiroyuki Fujiwara:** Supervision, Writing - review & editing.

Declaration of Competing Interest

The authors declare that they have no known competing financial interests or personal relationships that could have appeared to influence the work reported in this paper.

Acknowledgement

This work was supported by JSPS KAKENHI, Japan: Grant Number JP19H02167.

Data availability

The raw data required to reproduce these findings are available. The processed data required to reproduce these findings are also available.

Appendix A. Supplementary data

Supplementary data to this article can be found online at https://doi.org/10.1016/j.commatsci.2019.109315.

References

[1] Y. Hinuma, T. Hatakeyama, Y. Kumagai, L.A. Burton, H. Sato, Y. Muraba, S. Iimura, H. Hiramatsu, I. Tanaka, H. Hosono, F. Oba, Nat. Commun. 7 (2016) 11962.
[2] V.L. Shaposhnikov, A.V. Krivosheeva, V.E. Borisenko, J.-L. Lazzari, F. Arnaud d'Avitaya, Phys. Rev. B 85 (2012) 205201.
[3] W. Meng, B. Saparov, F. Hong, J. Wang, D.B. Mitzi, Y. Yan, Chem. Mater. 28 (2016) 821–829.
[4] M. Kato, T. Fujiseki, T. Miyadera, T. Sugita, S. Fujimoto, M. Tamakoshi, M. Chikamatsu, H. Fujiwara, J. Appl. Phys. 121 (2017) 115501.
[5] M. Gajdoš, K. Hummer, G. Kresse, J. Furthmüller, F. Bechstedt, Phys. Rev. B 73 (2006) 045112.
[6] C. Ambrosch-Draxl, J.O. Sofo, Comput. Phys. 175 (2006) 1–14.
[7] F. Kootstra, P.L. de Boeij, J.G. Snijders, Phys. Rev. B 62 (2000) 7071–7083.
[8] S. Botti, F. Sottile, N. Vast, V. Olevano, L. Reining, H.-C. Weissker, A. Rubio, G. Onida, R.D. Sole, R.W. Godby, Phys. Rev. B 69 (2004) 155112.
[9] J. Paier, M. Marsman, G. Kresse, Phys. Rev. B 78 (2008) 121201.
[10] H. Fujiwara, M. Kato, M. Tamakoshi, T. Miyadera, M. Chikamatsu, Phys. Status Solidi A 215 (2018) 1700730.
[11] J. Paier, R. Asahi, A. Nagoya, G. Kresse, Phys. Rev. B 79 (2009) 115126.
[12] C. Persson, J. Appl. Phys. 107 (2010) 053710.
[13] M. Nishiwaki, K. Nagaya, M. Kato, S. Fujimoto, H. Tampo, T. Miyadera, M. Chikamatsu, H. Shibata, H. Fujiwara, Phys. Rev. Mater. 2 (2018) 085404.
[14] K. Nagaya, S. Fujimoto, H. Tampo, S. Kim, M. Nishiwaki, Y. Nishigaki, M. Kato, H. Shibata, H. Fujiwara, Appl. Phys. Lett. 113 (2018) 093901.
[15] E.M. Chen, L. Williams, A. Olvera, C. Zhang, M. Zhang, G. Shi, J.T. Heron, L. Qi, L.J. Guo, E. Kioupakis, P.F.P. Poudeu, Chem. Sci. 9 (2018) 5405–5414.
[16] A. Nakane, H. Tampo, M. Tamakoshi, S. Fujimoto, K.M. Kim, S. Kim, H. Shibata, S. Niki, H. Fujiwara, J. Appl. Phys. 120 (2016) 064505.
[17] H. Fujiwara, R.W. Collins (Eds.), Spectroscopic Ellipsometry for Photovoltaics: Volume 2: Applications and Optical Data of Solar Cell Materials, Springer, Cham, 2018.
[18] J.P. Perdew, K. Burke, M. Ernzerhof, Phys. Rev. Lett. 77 (1996) 3865–3868.
[19] J. Wang, H. Chen, S.-H. Wei, W.-J. Yin, Adv. Mater. 31 (2019) 1806593.
[20] J. Heyd, G.E. Scuseria, M. Ernzerhof, J. Chem. Phys. 118 (2003) 8207–8215.
[21] J. Heyd, G.E. Scuseria, M. Ernzerhof, J. Chem. Phys. 124 (2006) 219906.
[22] M.P. Marder, Condensed Matter Physics, Wiley, Hoboken, 2010.
[23] M. Marsman, J. Paier, A. Stroppa, G. Kresse, J. Phys.: Condens. Matter 20 (2008) 064201.
[24] G. Kresse, J. Furthmüller, Phys. Rev. B 54 (1996) 11169–11186.
[25] H. Kageshima, K. Shiraishi, Phys. Rev. B 56 (1997) 14985–14992.
[26] Y. Zhang, X. Yuan, X. Sun, B.-C. Shih, P. Zhang, W. Zhang, Phys. Rev. B 84 (2011) 075127.
[27] M. Kato, M. Nishiwaki, H. Fujiwara, 2019, https://arxiv.org/abs/1906.03005.
[28] M. Shirayama, H. Kadowaki, T. Miyadera, T. Sugita, M. Tamakoshi, M. Kato, T. Fujiseki, D. Murata, S. Hara, T.N. Murakami, S. Fujimoto, M. Chikamatsu, H. Fujiwara, Phys. Rev. Appl. 5 (2016) 014012.
[29] S. Minoura, K. Kodera, T. Maekawa, K. Miyazaki, S. Niki, H. Fujiwara, J. Appl. Phys. 113 (2013) 063505.
[30] F. Gygi, A. Baldereschi, Phys. Rev. Lett. 62 (1989) 2160–2163.
[31] F. Bechstedt, Many-Body Approach to Electronic Excitations: Concepts and Applications, Springer, Heidelberg, 2015.